

УДК 620.9

Pioro I.¹, Zvorykina A.²

¹University of Ontario Institute of Technology, Faculty of Energy Systems and Nuclear Science.
Canada, Oshawa, Ontario

²National Technical University of Ukraine "Kiev Polytechnic Institute". Ukraine, Kiev

**SOME IMPORTANT ASPECTS FOR EXPERIMENTAL PAPERS:
PART 1. TYPICAL HEAT-TRANSFER / THERMALHYDRAULICS TEST FACILITY
AND PRACTICAL RECOMMENDATIONS FOR PERFORMING EXPERIMENTS**

Анотація

В першій частині статті описується типовий теплопередавальний/термогідрравлічний випробувальний пристрій для надкритичної вуглекислоти та надаються практичні рекомендації щодо виконання експериментів.

Abstract

This Part 1 of the paper describes a typical heat-transfer/thermalhydraulics test facility for

supercritical carbon dioxide and provides practical recommendations for performing experiments.

Introduction

Being a reviewer for many international journals, being a Track Chair for the International Conference On Nuclear Engineering (ICONE) and being an Associated Editor of the ASME Journal for Engineering on Gas Turbines and Power for a number of years we have found that many interesting and important experimental papers have been rejected by reviewers due to



lack of knowledge on specific requirements for this type of papers. The most important requirement is to provide complete information on uncertainties of measured and calculated parameters used in a paper. Many authors have completely ignored this requirement, but even if some of them have provided accuracies of sensors such as thermocouples, Resistor Temperature Detectors (RTDs), flowmeters, pressure transducers, etc., it was still not enough for paper acceptance. Therefore, in the current paper, which consists of 2 parts, we would like to present our vision on this issue and to provide readers with quite detailed information on uncertainty analysis as it was required by the nuclear industry. This paper is based on the test facility and experiments conducted so far in Chalk River Laboratories (CRL) Atomic Energy of Canada Limited (AECL). First part of the paper describes the test facility and the second one is actually the uncertainty analysis.

Glossary and definitions of selected terms and expressions related to critical and supercritical regions specifics

Prior to a general discussion on supercritical fluids, experimental facility and uncertainty analysis it is important to define special terms and expressions used at these conditions. For better understanding of these terms and expressions Figures A...D are shown below. Additional information on thermophysical-properties and heat-transfer specifics at critical and supercritical pressures can be found in Pioro et al. (2011), Pioro and Mokry (2011a, b), Mokry et al. (2011), Pioro (2008a, b), Pioro and Duffey (2007), and Pioro and Khartabil (2005).

Definitions of Selected Terms and Expressions Related to Critical and Supercritical Regions

Compressed fluid is a fluid at a pressure above the critical pressure, but at a temperature below the critical temperature (see Figures A and B).

Critical point (also called a *critical state*) is a point in which the distinction between the liquid and gas (or vapour) phases disappears, i.e., both phases have the same temperature, pressure and volume or density (see Figures A, B). The *critical point* is characterized by the phase-state parameters T_{cr} , P_{cr} and v_{cr} (or ρ_{cr}), which have unique values for each pure substance.

Deteriorated Heat Transfer (DHT) is characterized with lower values of the heat transfer coefficient compared to those at the normal heat transfer; and hence, has higher values of wall temperature within some part of a test section or within the entire test section (see Figures C and D).

Improved Heat Transfer (IHT) is characterized with higher values of the heat transfer coefficient compared to those at the normal heat transfer; and hence, lower values of wall temperature within some part of a

test section or within the entire test section. The improved heat-transfer regime or mode includes peaks or “humps” in the heat-transfer-coefficient profile near the critical or pseudocritical points (see Figure C).

Near-critical point is actually a narrow region around the critical point, where all thermophysical properties of a pure fluid exhibit rapid variations.

Normal Heat Transfer (NHT) can be characterized in general with values of the heat transfer coefficient similar to those at subcritical-pressure convective heat transfer, when they are calculated according to the conventional single-phase Dittus-Boelter-type correlations: $Nu = 0.023 Re^{0.8} Pr^{0.4}$ (see Figures C and D). Usually, the normal heat-transfer regime can be found far from the critical or pseudocritical regions.

Pseudo-boiling is a physical phenomenon similar to a subcritical-pressure nucleate boiling, which may appear at supercritical pressures. Due to heating of supercritical fluid with a bulk-fluid temperature below the pseudocritical temperature (high-density fluid, i.e., “liquid”), some layers near a heating surface may attain temperatures above the pseudocritical temperature (low-density fluid, i.e., “gas”). This low-density “gas” leaves the heating surface in the form of variable density (bubble) volumes. During the pseudo-boiling, the heat transfer coefficient usually increases (improved heat-transfer regime).

Pseudocritical line is a line, which consists of pseudocritical points (see Figures A and B).

Pseudocritical point (characterized with P_{pc} and T_{pc}) is a point at a pressure above the critical pressure and at a temperature ($T_{pc} > T_{cr}$) corresponding to the maximum value of the specific heat at this particular pressure (see Figures A and B).

Pseudo-film boiling is a physical phenomenon similar to subcritical-pressure film boiling, which may appear at supercritical pressures. At the pseudo-film boiling, a low-density fluid (a fluid at temperatures above the pseudocritical temperature, i.e., “gas”), prevents a high-density fluid (a fluid at temperatures below the pseudocritical temperature, i.e., “liquid”) from contacting (“rewetting”) a heated surface. Pseudo-film boiling leads to the deteriorated heat-transfer regime.

Supercritical fluid is a fluid at pressures and temperatures that are higher than the critical pressure and temperature (see Figures A and B). However, in the current paper, a term *supercritical fluid* includes both terms — a *supercritical fluid* and a *compressed fluid*.

Supercritical “steam” is actually supercritical water, because at supercritical pressures fluid is considered as a single-phase substance. However, this term is widely (and incorrectly) used in the literature in relation to supercritical “steam” generators and turbines.

Superheated steam is a steam at pressures below the critical pressure, but at temperatures above the critical temperature (see Figures A and B).

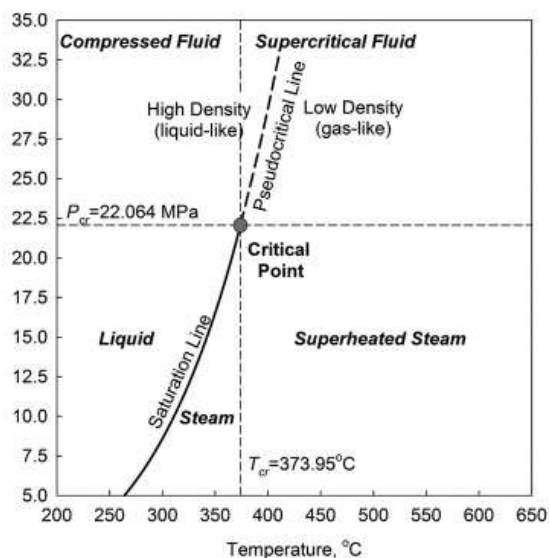


Fig. A. Pressure-Temperature diagram for water

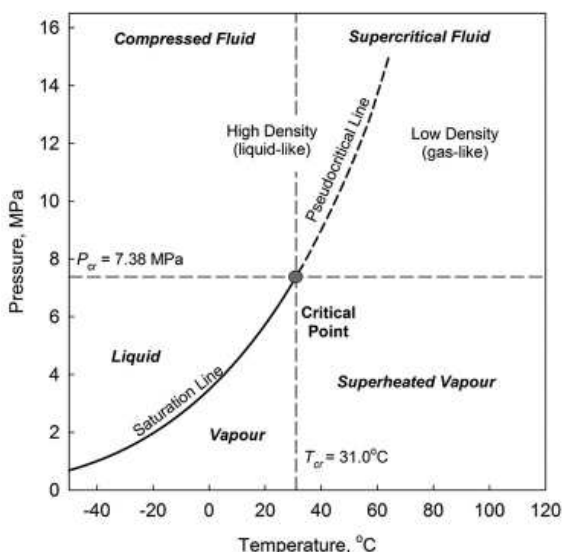


Fig. B. Pressure-Temperature diagram for carbon dioxide

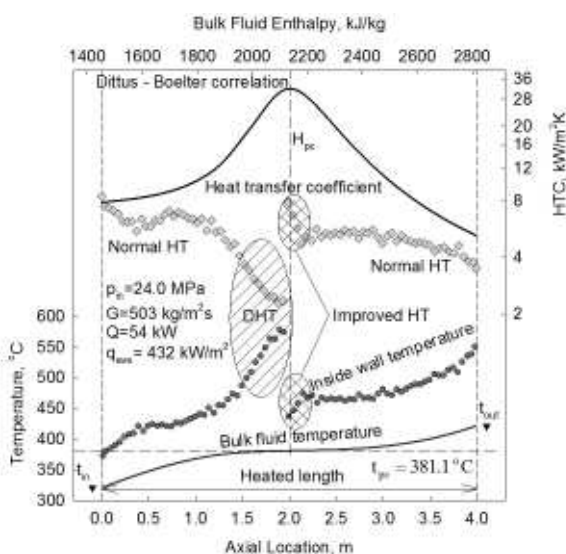


Fig. C. Temperature and heat-transfer-coefficient profiles along heated length of vertical circular tube (Kirillov et al., 2003): Water, $D = 10$ mm and $L_h = 4$ m

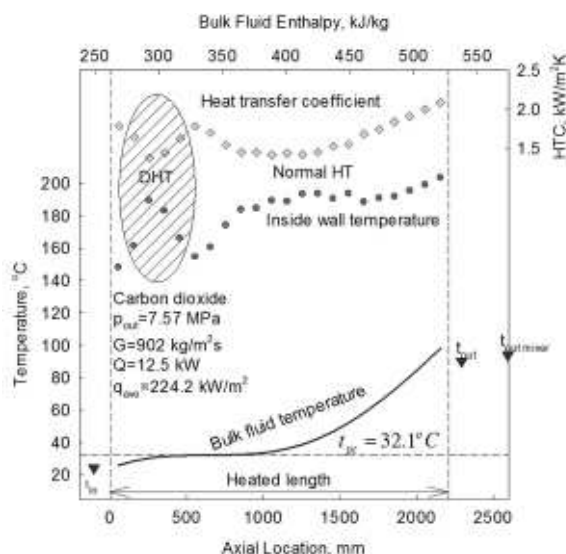


Fig. D. Temperature and heat-transfer-coefficient profiles along heated length of vertical circular tube: Carbon dioxide, $D = 8$ mm and $L_h = 2.208$ m

In general, carbon dioxide has been often used as a supercritical working fluid in various thermodynamic cycles and heat exchangers and as a modelling fluid instead of supercritical water, because of its lower critical pressure and temperature (see Table 1) (Piro, 2011a, b; 2010; Piro and Peiman, 2011; Piro and Duffey, 2007). Therefore, there is a significant interest to this modelling fluid, especially for SuperCritical Water-cooled Reactor's (SCWR's) application, because of high cost and technical difficulties in performing supercritical-water tests in bundle geometry. Also, using a modelling fluid such as CO₂ allows conducting experiments within a wider range of operating parameters than in water.

AECL at Chalk River Laboratories (CRL) has built a supercritical carbon dioxide loop to perform

Table 1

Critical parameters of water and CO₂ (NIST 2010)

Parameters	Unit	Water	CO ₂
Critical pressure	MPa	22.1	7.3773
Critical temperature	°C	374.1	31.0
Critical density	kg/m ³	315	467.6

preliminary heat-transfer and pressure-drop tests instead of supercritical water. Details of the CRL supercritical carbon-dioxide experimental setup are listed below.



Scaling Parameters

Scaling parameters used for modelling nominal supercritical-water operating conditions of the SCW CANDU reactor concept into supercritical carbon dioxide equivalent values are listed in Table 2. These scaling parameters (Piro and Duffey, 2007) were deduced from those originally proposed by Jackson and Hall (1979) and Gorban' et al. (1990).

Table 3 lists nominal operating parameters of the SCW CANDU reactor concept in water and carbon dioxide equivalent values.

Test Facility

Primary Recommendations

Recommendation 1. Put safety first: follow local safety codes, rules and regulations in an experimental-setup design, construction and operation.

Table 2
Basic scaling parameters for fluid-to-fluid modelling at supercritical conditions

Parameters	Scaling laws
Pressure	$\left(\frac{p}{p_{cr}}\right)_{CO_2} = \left(\frac{p}{p_{cr}}\right)_{Water}$
Bulk-fluid temperature (K)	$\left(\frac{T_b}{T_{cr}}\right)_{CO_2} = \left(\frac{T_b}{T_{cr}}\right)_{Water}$
Mass flux	$\left(\frac{GD}{\mu_b}\right)_{CO_2} = \left(\frac{GD}{\mu_b}\right)_{Water}$

Table 3
Nominal operating parameters of the SCW CANDU reactor concept and their equivalent values in CO₂

Parameters	Unit	Water	CO ₂
Operating pressure	MPa	25	8.34
Inlet temperature	°C	350	20
Outlet temperature	°C	625	150
Mass flux at inlet	kg/m ² s	1185	1630
Mass flux at outlet	kg/m ² s	1185	800

Recommendation 2. NIST (2010) thermophysical properties software is recommended for property calculations of various fluids (for details on NIST, see Appendix). Scaling parameters (see Table 2) can only be used for scaling operating conditions from one fluid to another for reference purposes. Due to scaling parameters simplicity, special behavior of thermophysical properties at supercritical pressures and complexity of

processes involved, some discontinuities may exist. For example, there can be a mass discontinuity, i.e., a value of the mass flux scaled at inlet conditions may not be the same as that scaled at outlet conditions (for details, see Table 2).

Heat flux has not been scaled, because it was proposed to change the heat flux from the minimal value to the maximum possible during the experiments.

Loop and CO₂ Supply

As a typical example, the MR-1 loop at the CRL (see Figure 1) is a high-temperature and high-pressure pumped loop. The operating pressure range is up to 10.3 MPa at temperatures up to 310 °C. The maximum mass-flow rate of supercritical carbon dioxide for the current tests is about 0.153 kg/s ($G = 3000 \text{ kg/m}^2\text{s}$ inside an 8-mm ID tube). Carbon dioxide (99.9 % purity, content of hydrocarbons 0.8 ppm) is charged into the loop from a tank installed outside the laboratory building. Power is delivered to the test section by a 350 kW (175 V × 2000 A) Direct-Current (DC) power supply.

Recommendation 3. DC power supply is more preferable for direct-heating applications compared to that of Alternative Current (AC), especially for thin-walled test sections¹. However, test-section surface temperature measurements with DC power supply will be more complicated, because they require insulating a thermocouple measuring tip from the electrically heated surface (for details, see below). With an AC power supply, a thermocouple-measuring tip may be in contact with an electrically heated surface as there is no average voltage offset across the probe junction. Nevertheless, special precautions should be taken to avoid spurious electromagnetic induction (emf), for example in a thermocouple wiring, which can be generated by a pulsating electromagnetic field around a test section.

Fluid passes from the pump through an orifice flowmeter, a preheater, a test section, a cooler and back to the pump. The centrifugal pump that circulates CO₂ through the loop is fitted with a special seal and barrier-fluid cooling system. This seal and fluid are needed to compensate for the poor lubricity of the CO₂.

Recommendation 4. A better solution for the circulation pump is a vertical canned-type pump manufactured by commercial suppliers, which does not require any lubrication and is suitable for many fluids within a wide range of pressures and temperatures. For lower mass-flow rates, an electromagnetic-driven head pump can be used.

¹ It was found that Critical Heat Flux (CHF) values at boiling obtained in or on a test section with DC direct heating can differ from those obtained in or on a test section with AC direct heating. This difference is larger for thin-walled test sections. At supercritical pressures, there is a similar phenomenon, which is called pseudo-boiling. Therefore, the above-mentioned findings may apply to the supercritical case.

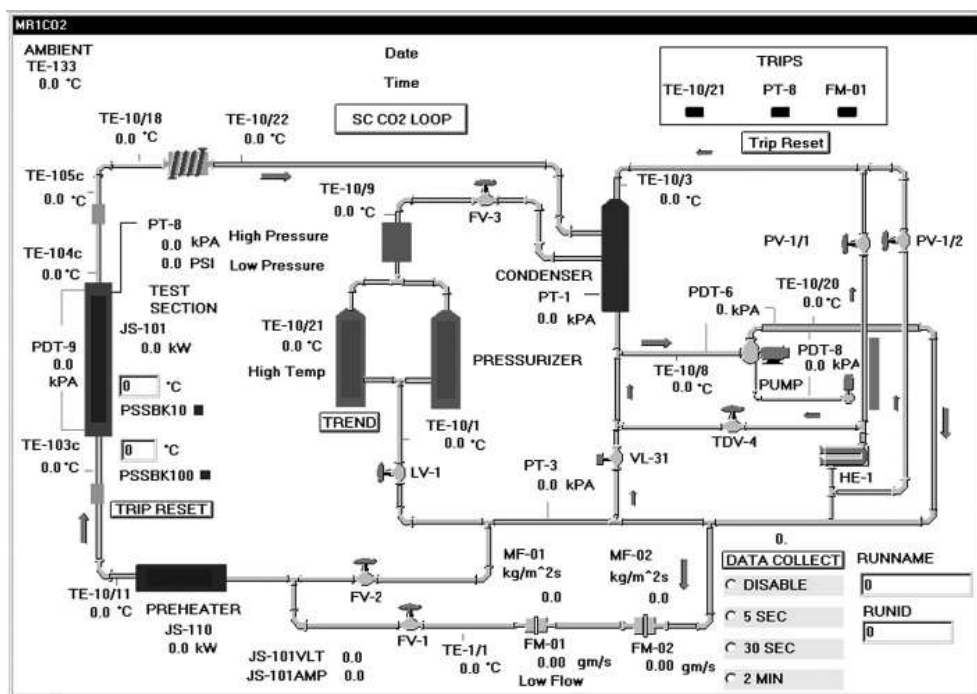


Fig. 1. SC CO₂ loop schematic (as shown on Data Acquisition System (DAS) display):

FM – flowmeter, FV – flow valve, HE – heat exchanger, JS – power, LV – level valve, MF – mass flux, PDT – pressure differential transducer, PSSBK – pressure set, PT – pressure transducer, PV – pressure valve, SC CO₂ – supercritical carbon dioxide, TDV – temperature difference valve, TE – temperature, and VL – valve for low flow

The CO₂ fluid passes through a 25-kW preheater into the test section. The preheater consists of electrically heated elements, installed in a pressure tube, that are controlled from the loop control panel.

Recommendation 5. To minimize thermal inertia and pressure drop of the preheater, the directly heated tube or tubes can be used with an additional power supply.

Cooling is achieved just downstream of the test section using helicoil coolers or heat exchangers (the coolant is near-ambient temperature river water). The temperature of the river water varies between 4 and 20°C, depending on the season.

Recommendation 6. For CO₂ application, lower inlet temperatures may be required, so a refrigeration unit may be needed in the cooling system.

While some of the heat from the test section can be removed using the small helicoil coolers, large amounts are removed using the main loop heat exchanger in the discharge circuit of the pump. Pressurization is achieved by applying an electrical power to the heating elements in two vessels. Pressure is controlled automatically from the panel by using the outlet test-section pressure (PT-8) as a set point for regulating the power input to the heating elements.

Recommendation 7. Pressurization with electrically heated elements installed inside a pressure vessel is more preferable than the pressurization with an inert gas through a membrane or with a direct contact

between the gas and the loop working fluid. The volume of the vessel should be at least several times larger than the loop total internal volume to assure stable pressure during operation.

Test matrix is listed in Table 4.

Test-Section Design

The test section was installed vertically with an upward flow of carbon dioxide. The current test-section

Table 4

Test matrix

No of points	p_{out} , MPa	G , kg/m ² s	t_{in} , °C	t_{out} , °C	q , kW/m ²
158	7.36	900, 2000	25, 30	29...82	37...447
129	8.36	2000	21	29...94	115...48
664		295...2060	21...30	35...124	16...225
598		900, 2780...3200	25...40	32...139	27...616
416		1500, 2020	30...40	33...131	30...460
581		784...2000	20...40	39...120	221...46
182		750	31...40	35...136	18...209
108	8.8	900, 2000	31	37...107	28...225
181	8.83	2002, 3020	30	35...89	30...536

design (see Figure 2) consists of a 2.4-m-long tubular section of 8-mm ID Inconel-600 tubing with a 2.208-m heated length (for additional information on the test section, see Piro and Duffey, 2007). The diameter is close to the hydraulic-equivalent diameter of a typical subchannel in a 43-element fuel bundle that is considered for use in the SCW CANDU reactor.

Recommendation 8. It is unlikely that a simple circular geometry can fully model a thermalhydraulic behavior of any actual subchannel geometry. However, it is a good practice to have a tube ID close to a hydraulic-equivalent diameter of the average subchannel; and a tube heated length equals to that of a fuel bundle.

The fluid is heated by means of a direct electrical current passing through the tube wall from the inlet to the outlet power terminals (copper clamps).

Recommendation 9. In general, an electrical resistance of the heated part of the test section should be equal to or at least to be close to the nominal electrical resistance of the power supply, i.e., for example, for the typical power supply – $R_{el}^{TS} = R_{el}^{nom} = 175 \text{ V} / 2000 \text{ A} = 0.0875 \text{ Ohm}$. Only in this particular case, the nominal power of the

power supply (i.e., 350 kW) can be applied to the test section. Otherwise, the limiting factors on the applied power will be the nominal voltage of the power supply (175 V) if $R_{el}^{TS} > R_{el}^{nom}$ or the nominal current (2000 A) if $R_{el}^{TS} < R_{el}^{nom}$. The power deposited in the test section can be compared to the loop heat balance from the known flow and enthalpy (temperature rise) across the test section.

Recommendation 10. Material for a directly heated test section should be chosen with a relatively high value of the specific electrical resistivity, which in turn should ideally be invariant or nearly independent of wall temperature. In this case, there is a wider range for changing the test-section wall thickness and heated length. Also, the local heat flux will be more uniform along the test section in spite of variable wall temperature if the test-section diameter and wall thickness are constant along the heated length. Therefore, Inconel 600 or Inconel 718 will be the best choice for material of the test section (Figure 3). Additional characteristics of the test section, such as the chemical content, precise measurements of the inside/outside tube diameters, the tube burst pressure, tube electrical resistance, and the electrical resistivity and thermal conductivity of the tube material are also essential for the complete performance and safety analysis.

Recommendation 11. For a uniform temperature profile in a cross section of the test section at the inlet and for accurate bulk-fluid temperature measurements, mixing chambers should be used together with sheathed thermocouples installed just downstream of them. It is especially important for supercritical pressures applications. Also, between the inlet mixing chamber and the test section the flow stabilization part should be installed with the same diameter as that of the test section, acting as a settling length. In general, the length of this part should be about $(20...50) \cdot D$. The outlet mixing chamber should be installed just downstream of the test-section outlet to reduce uncertainties in the outlet bulk-fluid temperature measurement, and hence, in the loop heat balance.

Recommendation 12. The test section (see Figure 2) and mixing chambers should be wrapped with thermal insulation to minimize heat loss.

Instrumentation

The following test-section parameters were measured during the experiment (see Figures 1 and 2):

- The test-section current (the current was calculated using a measured voltage drop on a calibrated shunt) and voltage (to give power, JS-101).
- The pressure at the test section outlet (PT-8).
- Four pressure drops over equal lengths (536 mm) along the test section (PDT-110 to PDT-113), and an overall test-section pressure drop (PDT-9).
- Temperatures at the test-section inlet and outlet (TE-103, TE-104 and TE-105).

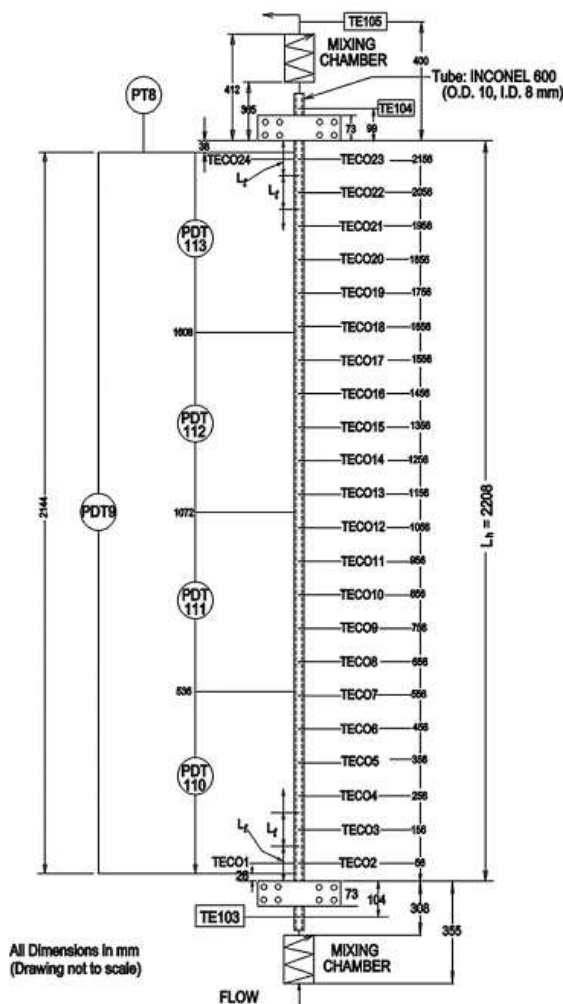


Fig. 2. SC CO₂ test-section thermocouples and pressure-taps layout

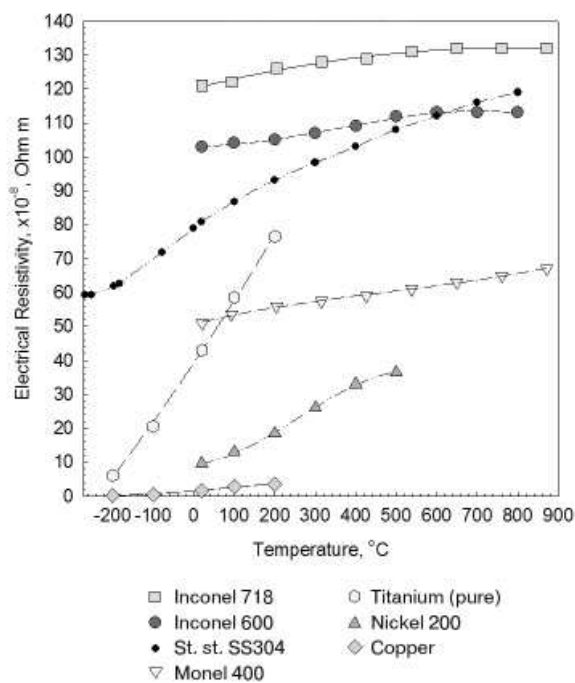


Fig. 3. Effect of temperature on electrical resistivity of alloys and pure metals

- Wall temperatures at equal intervals² (100 mm) along the test section (TECO1 to TECO24).
- The CO₂ mass-flow rate.
- The ambient temperature.

Measurement uncertainties for all instruments are listed in Table 5.

It was decided to provide a sample of the actual uncertainty analysis (for details, see Part 2 of this paper) in this paper because, usually, only simple examples of uncertainty calculations can be found in the open literature.

The total test-section power is a calculated value that is based on the measured values of current and voltage drop across the test section.

The test section has equally spaced pressure taps for pressure loss readings (see Figure 2), which allows determination of the test-section local and total pressure drops.

The sum of the local pressure drops measured with PDT-110 – PDT-113 was used to check the total test-section pressure drop measurement from PDT-9 for an instrument consistency.

The test-section inlet and outlet bulk-fluid temperatures (TE-103, TE-104 and TE-105) are measured using 1/16" K-type ungrounded sheathed thermocouples inserted into the fluid stream (see Figures 1 and 2). The thermocouples are used with electronic-reference units. Also, the thermocouples were calibrated *in situ*, i.e., by comparing the reading on the DAS with the calibration standard (for measurement uncertainties, see Part 2 of

² Smaller pitch is recommended. A pitch of 50 mm is reasonable in this case.

Table 5
Selected uncertainties of measured and calculated parameters
(for details, see Part 2 of this paper)

Parameters	Uncertainty
Test-section power/heat flux	±0.5%
Inlet/outlet pressure	±0.2%
Local pressure drops	±0.8% at $\Delta P = 30$ kPa ±5.0% at $\Delta P = 5$ kPa
Bulk-fluid and wall temperatures	±0.3°C within 0...100°C ±2.2°C beyond 100°C
Mass-flow rate/mass flux	±1.6% at $m = 155$ g/s ($G = 3084$ kg/m ² s) ±12.5% at $m = 46$ g/s ($G = 915$ kg/m ² s)

this paper). Therefore, the appropriate temperature-dependent correction was applied to each temperature value measured by thermocouples within the calibration temperature range of 0...100°C. Beyond this temperature range, no temperature corrections were applied to the measured temperature values.

Recommendation 13. Calibration of various measuring instruments *in situ* is the best way to minimize measurement uncertainties compared to other calibration techniques (calibration at an instrument shop, calibration check, etc.), because a calibration curve will take care of uncertainties of measuring, signal transmitting, signal converting devices, etc. (for details, see Part 2 of this paper).

To measure the enthalpy increase, thermocouples TE-103 and TE-105 (see Figures 1 and 2) are installed just downstream of the mixing chambers. To assess an impact of the mixing chambers, an additional thermocouple TE-104 was installed just downstream of the test section but upstream of the outlet mixing chamber.

Recommendation 14. For bulk-fluid temperature measurements, Resistance Temperature Detectors (RTDs) are more preferable to use compared to thermocouples, because they are usually more accurate. However, it is a good practice to use thermocouples in addition to RTDs as the back-up temperature devices.

For wall temperature estimates, twenty-four fast-response K-type thermocouples with self-adhesive fiberglass backing were attached to the tube outer wall at equal intervals of 100 mm (see Figure 2). The thermocouples were additionally secured by wrapping them with Teflon tape and fiberglass string to achieve proper contact with the wall. The fiberglass backing could withstand temperatures of up to 260°C for extended periods of time and up to 370°C for a short duration. Therefore, the temperature trip for the external-wall temperature was set at 250°C. Thermocouples TECO2 to TECO23 are located on one side of the test section. Thermocouples TECO1 and TECO24 are located in the



same cross sections as the thermocouples TECO2 and TECO23, but 180° apart.

Recommendation 15. For relatively low wall-temperature measurements, i.e., up to 260°C, fast-response thermocouples are the easiest way to go. However, beyond this range sheathed ungrounded thermocouples should be used welded to a surface and calibrated in situ. This recommendation applies to flow geometry cooled from inside (circular tubes, etc.).

Loop Control, Data Acquisition and Processing

Modern DAS are all computer based. Personal Computer (PC) software is used for trip control, together with a Programmable Logic Controller (PLC). The trips are intended to enhance protection to the personnel and equipment in the event of system malfunctions. The trips are selected for a high pressure, high temperature and low flow. The PLC provides power trips to the pressurizer heaters, the preheater, the test-section power supply, the pump and the test-section shutoff valves. An operator can program trip set points into the DAS.

Recommendation 16. Always use multiple trips setup in DAS for safe and reliable test facility operation.

Recommendation 17. Do not rely solely on a DAS and other electronic measuring devices, but also use, in parallel, simple devices for measuring or just for indication of the most important/safety/limiting parameters: for example, high-accuracy mechanical gauges (for pressure), arrow-type voltmeters and ammeters, plus use remote video cameras for monitoring heated parts of a test section, pumps, etc.

Figure 1 shows a typical DAS display that is available to an experimenter and operator during the loop operation. For steady-state testing, at constant flow and power, data can be collected every five seconds during a one-minute scan. However, data on the screen were updated every second. Data were retrieved and converted into an EXCEL (.xls) file format for post-test processing.

Quality Assurance

To ensure the accuracy of the experimental data:

– Instruments (thermocouples, pressure transmitters and Differential Pressure (DP) cells) were calibrated by qualified instrument technicians using traceable standards.

– DAS-to-instrument connections and data storage were verified.

– Calibration records for instrumentation are stored in a filing cabinet.

Conduct of Tests

To establish a heat balance, a heat-loss test with power applied to the test section (the loop is vacuumed) was conducted (for details, see Part 2 of this paper). Such test is more accurate compared to that with the zero power (i.e., test based on heat-balance technique, when hot fluid is cooled flowing through a test section;

power are not applied to the test section), because it eliminates uncertainties that are related to an estimation of the thermophysical properties of CO₂. This test also eliminates flow-measurement uncertainties and uncertainties that are incurred when measuring very small temperature differences (0.5...1°C) between inlet and outlet bulk-fluid temperatures.

Based on these heat-loss tests, it was concluded that heat loss from the test section was small, i.e., about 0.4% at the highest wall-to-ambient temperature difference of 220°C in the SC CO₂ loop. Nevertheless, the power used in the heat-transfer calculations was adjusted for the heat loss.

The experimental data were recorded by the DAS when the desired flow conditions and power level were reached and stabilized. Operating conditions that were judged to be steady are as follows:

- Outlet-pressure fluctuations were within $\pm 0.2\%$.
 - Mass-flux fluctuations were generally within $\pm 1.0\%$ (in several cases, they fluctuated up to $\pm 1.7\%$).
 - Heat-flux fluctuations were within $\pm 0.2\%$.
 - Inlet-temperature fluctuations were generally within $\pm 1.0\%$ (in several cases, they fluctuated up to 1.5%).
 - External wall-temperature fluctuations were within $\pm 0.7\%$.
 - Pressure-drop fluctuations were generally within $\pm 2.0\%$ (in several cases, they fluctuated up to $\pm 2.8\%$).
- The data were recorded³ over one minute in five-second intervals.

The test procedure was as follows:

1. Increase the loop pressure with electrical heaters to the required value.
2. Start the circulation pump and establish the required mass-flow rate by adjusting the regulating valve installed just upstream of the test section.
3. Use the preheater to establish the required inlet temperature.
4. Adjust all controlled parameters – pressure, mass-flow rate and inlet temperature (for adjustment details, see steps 1 to 3) – to the required nominal values (if needed).
5. Start the power supply and establish the required power level by increasing power in small increments.
6. Read just all controlled parameters (see Step 4) to the required nominal values (if needed).
7. Monitor measured parameters via the DAS display. When steady-state conditions are achieved, scan all data in five-second intervals over a one-minute period.
8. Repeat steps 3 to 7 for other flow conditions.

Data Reduction

The data-reduction procedure is based on local parameters, which were measured or calculated at each

³ Input signals from all 64 channels were read over a period of 10 ms.

cross section (or vertical elevation) corresponding to the external-wall thermocouples. The external-wall temperatures, inlet and outlet bulk-fluid temperatures and electrical current were used as the basis for local-parameter calculations. These local parameters include thermal conductivity and electrical resistivity of the wall material, electrical resistance, power, heat flux, volumetric heat flux, internal wall temperature, heat loss, bulk-fluid temperature and pressure.

It should be noted that when the measured inlet bulk-fluid temperature is close to pseudocritical or critical temperatures, the value of inlet temperature *cannot be reliably used* as the starting point for downstream bulk-fluid temperature calculations. There are significant variations in thermophysical properties near the pseudocritical and critical points, which lead to increased uncertainties in calculations (for additional information, see Part 2 of this paper). Therefore, a value of the measured test-section outlet bulk-fluid temperature should be used for upstream bulk-fluid temperature calculations instead of the inlet bulk-fluid temperature.

The same explanation applies to the temperature on which fluid density for the flow-rate calculation is based, i.e., thermocouple TE-1/1 located near the orifice-plate flowmeter. In this case, this temperature should be below or beyond the critical or pseudocritical temperature regions.

The general and local parameters are defined as follows:

General parameters:

– Flow area: $A_{fl} = \pi D^2/4$, where D is the inside tube diameter.

– Mass flux: $G = m/A_{fl}$, where m is the mass-flow rate.

– Total heated area: $A_h = \pi DL$, where L is the total heated length.

– Measured power: $POW = UI$, where U is the test-section voltage drop, and I is the electrical current.

– Average heat flux: $q = (POW - HL)/A_h$.

– Inlet pressure: $p_{in} = p_{out} + \Delta p_{TS}$, where Δp_{TS} is the total pressure drop across the test section.

– Thermophysical properties of carbon dioxide: fluid density, specific heat, enthalpy, thermal conductivity, and dynamic viscosity. These properties were calculated using NIST software (2010). The thermophysical properties at a particular cross section were calculated based on the local pressure and local bulk-fluid temperature. The pseudocritical temperature was evaluated at the outlet pressure. However, there is a range of pseudocritical temperatures for each set of flow conditions along the test section, because t_{pc} depends on pressure and pressure changes from the inlet to the outlet. Nevertheless, the changes in pseudocritical temperature are small (less than 0.6°C) within the heated length of 2.2 m. For example, within the range of pressures $p_{in} = 8.3\text{ MPa}$ and $p_{out} = 8.4\text{ MPa}$, i.e.,

$\Delta p_{TS} = 100\text{ kPa}$, the difference in pseudocritical temperature is only $\Delta t_{pc} = 0.55^\circ\text{C}$.

Local parameters:

– Heated area: $A_{h,l} = \pi DL_1$, where L_1 is the local heated length (see Figure 2). For thermocouples TECO3 to TECO22 the local heated length is 100 mm, for TECO1 and TECO2 it is 106 mm and for TECO23 and TECO24 it is 102 mm. It was assumed that within the local heated length the external wall temperature is constant and equals the value measured by wall thermocouples.

– Power⁴: $POW_1 = I^2 \cdot R_{el,1}$, where $R_{el,1}$ is the local electrical resistance⁵ within the local heated length calculated using a local value of electrical resistivity.

– Heat flux: $q_1 = (POW_1 - HL_1)/A_{h,1}$, where HL_1 is the local heat loss based on the corresponding external wall-temperature measurements. There is a minor change in axial heat flux due to direct heating and the effect of wall temperature on electrical resistivity of material. Inconel 600, which has one of the weakest effects of temperature on electrical resistivity, was used as the test section material to minimize this effect.

– Tube wall thermal conductivity ($k_{w,1}$) was calculated using the average wall temperature $t_w^{ave} = (t_w^{ext} + t_w^{int})/2$.

– Volumetric heat flux: $q_{v,1} = \frac{POW_1}{\frac{\pi}{4}(D_{ext}^2 - D^2)L_1}$.

– Internal wall temperature:

$$t_w^{int} = t_w^{ext} + \frac{q_{v,1}}{4k_{w,1}} \left[\left(\frac{D_{ext}}{2} \right)^2 - \left(\frac{D}{2} \right)^2 \right] - \frac{q_{v,1}}{2k_{w,1}} \left(\frac{D_{ext}}{2} \right)^2 \ln \frac{D_{ext}}{D}.$$

This equation accounts for the uniformly distributed heat-generating sources inside the tube wall, i.e., heating with direct current passing through the tube wall.

– Local pressure: $p_1 = p_{in} - \frac{\Delta p_{PDT110}}{536} \cdot (z_{TECO_n} - 26)$,

where z is the external wall thermocouple location in mm from the beginning of the heating zone, $n = 1..7$ and is the thermocouple number. For thermocouples TECO8 – TECO12:

$$p_1 = p_{in} - \Delta p_{PDT110} - \frac{\Delta p_{PDT111}}{536} \cdot z_{TECO_n}, \text{ where } n = 8..12.$$

The same approach is applied to other thermocouples.

– Local inlet bulk-fluid enthalpy is calculated through the NIST software (2010) using the measured inlet temperature and the calculated inlet pressure.

⁴ Sum of local powers were checked against the total power applied to the test section for each run, to ensure that these values do not differ significantly. In general, the difference was within 2.5%.

⁵ Sum of $R_{el,1}$ was checked against the value of the total electrical resistance of the test section, calculated as U_{TS}/I , for each run, to ensure that these values do not differ significantly. In general, this difference was within 2.5%.



– Local bulk-fluid enthalpies in the cross section, where the external wall thermocouples were located, are calculated using the heat-balance method:

$$H_{b,l}|_{i+1} = H_{b,l}|_i + \frac{POW_l - HL_l}{m}$$

– Local bulk-fluid temperature (t_b) was calculated through the NIST software (2010) using the local pressure and local enthalpy in the cross section, where the external wall thermocouples were located.

$$\text{– Local HTC: } HTC_l = \frac{q_l}{t_w^{\text{int}} - t_b}$$

Sample of experimental data obtained at this test facility is shown in Figure D and more data are shown in Piro and Duffey (2007) and Piro and Khartabil (2005).

A detailed uncertainty analysis is listed in Part 2 of this paper.

Nomenclature

A	area, m ² ;
A_{fl}	flow area, m ² ;
A_h	total heated area;
c_p	specific heat at constant pressure, J/kg K;
c_v	specific heat at constant volume, J/kg K;
D	inside diameter, m;
G	mass flux, kg/m ² s $\left(\frac{m}{A_{fl}} \right)$;
H	specific enthalpy, J/kg;
HL	heat loss, W;
HTC_l	local heat transfer coefficient;
I	current, A;
k	thermal conductivity, W/m K;
L	heated length, m;
m	mass-flow rate, kg/s;
P, p	pressure, MPa;
POW	power, W;
Q	power or heat-transfer rate, W;
q	heat flux, W/m ² $\left(\frac{Q}{A_h} \right)$;
q_v	volumetric heat flux, W/m ³ $\left(\frac{Q}{V_h} \right)$;
R_{el}	electrical resistance, Ohm;
T, t	temperature, °C;
U	voltage, V;
V	volume, m ³ ;
v	specific volume, m ³ /kg;
z	axial coordinate, m

Subscripts or superscripts

ave	average;
b	bulk;
cr	critical;

el	electrical;
ext	external;
fl	flow;
h	heated;
in	inlet;
int	internal;
l	local;
nom	nominal or normal;
out	outlet or outside;
pc	pseudocritical;
TS	test section;
v	volumetric;
w	wall

Greek Letters

α	thermal diffusivity, m ² /s $\left(\frac{k}{c_p \rho} \right)$;
Δ	difference;
μ	dynamic viscosity, Pa · s

Non-dimensional Numbers

Nu	Nusselt number $\left(\frac{h D}{k} \right)$;
Pr	Prandtl number $\left(\frac{\mu c_p}{k} \right) = \left(\frac{\nu}{\alpha} \right)$;
Re	Reynolds number $\left(\frac{GD}{\mu} \right)$

Abbreviations and acronyms

AC	Alternating Current;
AECL	Atomic Energy of Canada Limited (Canada);
ASME	American Society of Mechanical Engineers;
CANDU	CANada Deuterium Uranium nuclear reactor;
CHF	Critical Heat Flux;
CRL	Chalk River Laboratories, AECL (Canada);
DAS	Data Acquisition System;
DC	Direct Current;
DHT	Deteriorated Heat Transfer;
DP	Differential Pressure;
HT	Heat Transfer;
HTC	Heat Transfer Coefficient;
ICONE	International Conference On Nuclear Engineering;
ID	Inside Diameter;
IHT	Improved Heat Transfer;
NHT	Normal Heat Transfer;
NIST	National Institute of Standards and Technology (USA);
PC	Personal Computer;
PDT	Pressure Differential Transducer;
PLC	Programmable Logic Controller;

PT	Pressure Transducer;
RTD	Resistance Temperature Detector;
SCW	SuperCritical Water;
SCWR	SuperCritical Water-cooled Reactor;
TE	Temperature;
UOIT	University of Ontario Institute of Technology;
US or USA	United States of America

References

1. *Gorban', L.M., Pomet'ko, R.S. and Khryashev, O.A., 1990. Modeling of water heat transfer with Freon of supercritical pressure, (In Russian), ФЭИ-1766, Institute of Physics and Power Engineering (ФЭИ), Obninsk, Russia, 19 pages.*

2. *Jackson, J.D. and Hall, W.B., 1979. Forced convection heat transfer to fluids at supercritical pressure, In book: Turbulent Forced Convection in Channels and Bundles, Editors S. Kakaç and D.B. Spalding, Hemisphere Publishing Corp., New York, NY, USA, Vol. 2, pp. 563–612.*

3. *Mokry, S., Pioro, I.L., Farah, A., King, K., Gupta, S., Peiman, W. and Kirillov, P., 2011. Development of Supercritical Water Heat-Transfer Correlation for Vertical Bare Tubes, Nuclear Engineering and Design, Vol. 241, pp. 1126–1136.*

4. *NIST Reference Fluid Thermodynamic and Transport Properties – REFPROP, 2010. NIST Standard Reference Database 23, Ver. 9.0, E.W. Lemmon, M.L. Huber and M.O. McLinden, National Institute of Standards and Technology, Boulder, CO, U.S. Department of Commerce, December.*

5. *Pioro, I., 2011a. The Potential Use of Supercritical Water-Cooling in Nuclear Reactors. Chapter in Nuclear Energy Encyclopedia: Science, Technology, and Applications, Editors: S.B. Krivit, J.H. Lehr and Th.B. Kingery, J. Wiley & Sons, Hoboken, NJ, USA, pp. 309–347 pages.*

6. *Pioro, I., 2011b. Nuclear Power as a Basis for Future Electricity Production in the World: Part 1. Generation III and IV Reactors, Technological Systems (Ukraine), Vol. 3 (56), pp. 20–37.*

7. *Pioro, I., 2010. Generation IV Nuclear Reactors: Supercritical Water-Cooled Reactor Concept, Technological Systems (Ukraine), Vol. 1 (50), pp. 74–82.*

8. *Pioro, I.L., 2008a. Thermophysical Properties at Critical and Supercritical Pressures, Section 5.5.16 in Heat Exchanger Design Handbook, Begell House, New York, NY, USA, 14 pages.*

9. *Pioro, I.L., 2008b. Heat Transfer to Supercritical Fluids, Section 2.2.10 in Heat Exchanger Design Handbook, Begell House, New York, NY, USA, 19 pages.*

10. *Pioro, I.L. and Duffey, R.B., 2007. Heat Transfer and Hydraulic Resistance at Supercritical Pressures in*

Power Engineering Applications, ASME Press, New York, NY, USA, 334 pages.

11. *Pioro, I.L. and Khartabil, H.F., 2005. Experimental Study on Heat Transfer to Supercritical Carbon Dioxide Flowing Upward in a Vertical Tube, Proc. of the 13th Int. Conf. on Nuclear Engineering (ICONE-13), Beijing, China, May 16–20, Paper #50118, 9 pages.*

12. *Pioro, I. and Mokry, S., 2011a. Thermophysical Properties at Critical and Supercritical Conditions, Chapter in book “Heat Transfer. Theoretical Analysis, Experimental Investigations and Industrial Systems”, Editor: A. Belmiloudi, INTECH, Rijeka, Croatia, pp. 573–592.*

13. *Pioro, I. and Mokry, S., 2011b. Heat Transfer to Fluids at Supercritical Pressures, Chapter in book “Heat Transfer. Theoretical Analysis, Experimental Investigations and Industrial Systems”, Editor: A. Belmiloudi, INTECH, Rijeka, Croatia, pp. 481–504.*

14. *Pioro, I., Mokry, S. and Draper, Sh., 2011. Specifics of Thermophysical Properties and Forced-Convective Heat Transfer at Critical and Supercritical Pressures, Reviews in Chemical Engineering, Vol. 27, Issue 3–4, pp. 191–214.*

15. *Pioro, I. and Peiman, W., 2011. Nuclear Power as a Basis for Future Electricity Production in the World: Part 2. Supercritical Water-Cooled Reactor Concept, Technological Systems (Ukraine), Vol. 4 (57), pp. 19–31.*

Appendix

The NIST REFPROP Version 9.0⁶ (2010) includes 105 pure fluids, 5 pseudo-pure fluids (such as air) and mixtures with up to 20 components:

– The typical natural gas constituents methane, ethane, propane, butane, isobutane, pentane, isopentane, hexane, isohexane, heptane, octane, nonane, decane, dodecane, carbon dioxide, carbon monoxide, hydrogen, nitrogen, and water.

– The hydrocarbons acetone, benzene, butene, cis-butene, cyclohexane, cyclopentane, cyclopropane, ethylene, isobutene, methylcyclohexane, propylcyclohexane, neopentane, propyne, trans-butene, and toluene.

– The HFCs (Hydro-Fluoro-Carbons) R-23, R-32, R-41, R-125, R-134a, R-143a, R-152a, R-161, R-227ea, R-236ea, R-236fa, R-245ca, R-245fa, R-365mfc, R-1234yf, and R-1234ze(E).

– The HCFCs (Hydro-Chloro-Fluoro-Carbons) R-21, R-22, R-123, R-124, R-141b, and R-142b.

– The traditional CFCs (Chloro-Fluoro-Carbons) R-11, R-12, R-13, R-113, R-114, and R-115.

– The FCs (Fluoro-Carbons) R-14, R-116, R-218, C4F10, C5F12, and RC-318.

⁶ Information on the NIST REFPROP software is taken from <http://www.nist.gov/srd/nist23.cfm>.



– The “natural” refrigerants ammonia, carbon dioxide, propane, isobutane, and propylene.

– The main air constituents nitrogen, oxygen, and argon.

– The noble elements helium, argon, neon, krypton, and xenon.

– The cryogenics argon, carbon monoxide, deuterium, krypton, neon, nitrogen trifluoride, nitrogen, fluorine, helium, methane, oxygen, normal hydrogen, parahydrogen and orthohydrogen.

– Water (as a pure fluid, or mixed with ammonia).

– Miscellaneous substances including carbonyl sulfide, dimethyl carbonate, dimethyl ether, ethanol, heavy water, hydrogen sulfide, methanol, nitrous oxide, sulfur hexafluoride, sulfur dioxide, and trifluoroiodomethane.

– The FAMES (Fatty Acid Methyl Esters, i.e., biodiesel constituents): methyl oleate, methyl palmitate, methyl stearate, methyl linoleate, and methyl linolenate.

– The siloxanes: octamethylcyclotetrasiloxane, decamethylcyclopentasiloxane, dodecamethylcyclohexa-

siloxane, decamethyltetrasiloxane, dodecamethylpentasiloxane, tetradecamethylhexasiloxane, octamethyltrisiloxane, and hexamethyldisiloxane.

– 67 predefined mixtures (such as R407C, R410A, and air); the user may define and store others.

Available properties

Temperature, Pressure, Density, Energy, Enthalpy, Entropy, c_v , c_p , Sound Speed, Compressibility Factor, Joule Thompson Coefficient, Quality, 2nd and 3rd Virial Coefficients, 2nd and 3rd Acoustic Virial Coefficients, Helmholtz Energy, Gibbs Energy, Heat of Vaporization, Fugacity, Fugacity Coefficient, Chemical Potential, K value, Molar Mass, B12, Thermal Conductivity, Viscosity, Kinematic Viscosity, Thermal Diffusivity, Prandtl Number, Surface Tension, Dielectric Constant, Gross and Net Heating Values, Isothermal Compressibility, Volume Expansivity, Isentropic Coefficient, Adiabatic Compressibility, Specific Heat Input, Exergy, Gruneisen, Critical Flow Factor, Excess Values, dp/dr , d^2p/dr^2 , dp/dT , dr/dT , dr/dp , and many others.